Frontiers of Information Technology & Electronic Engineering
www.jzus.zju.edu.cn; engineering.cae.cn; www.springerlink.com
ISSN 2095-9184 (print); ISSN 2095-9230 (online)
E-mail: jzus@zju.edu.cn

Optimal design of a large dual-polarization microstrip reflectarray with China-coverage patterns for satellite communications*

Gang ZHAO, Yong-chang JIAO‡, Guan-tao CHEN

National Key Laboratory of Antennas and Microwave Technology, Xidian University, Xi'an 710071, China

E-mail: gangzhao@mail.xidian.edu.cn; ychjiao@xidian.edu.cn; gtchen@stu.xidian.edu.cn

Received Sept. 16, 2019; Revision accepted Dec. 22, 2019; Crosschecked Jan. 18, 2020

Abstract: A large dual-polarization microstrip reflectarray with China-coverage patterns in two operating bands is designed. To sufficiently compensate for the spatial phase delay differences in two operating bands separately, a three-layer rectangular patch element is addressed, which is suitable for the large dual-polarization reflectarray. Due to the complexly shaped areas and high gain requirements, there are more than 25 000 elements in the reflectarray, making it difficult to design, due to more than 150 000 optimization variables. First, the discrete fast Fourier transform (DFFT) and the inverse DFFT are used to establish a one-to-one relationship between the aperture distribution and the far field, which lays a foundation for optimizing the shaped-beam reflectarray. The intersection approach, based on the alternating projection, is used to obtain the desired reflection phases of all the elements at some sample frequencies, and a new method for producing a suitable initial solution is proposed to avoid undesired local minima. To validate the design method, a dual-polarization shaped-beam reflectarray with 7569 elements is fabricated and measured. The measurement results are in reasonable agreement with the simulation ones. Then, for the large broadband reflectarray with the minimum differential spatial phase delays in the operating band, an approach for determining the optimal position of the feed is discussed. To simultaneously find optimal dimensions of each element in two orthogonal directions, we establish a new optimization model, which is solved by the regular polyhedron method. Finally, a dual-band dual-polarization microstrip reflectarray with 25 305 elements is designed to cover the continent of China. Simulation results show that patterns of the reflectarray meet the China-coverage requirements in two operating bands, and that the proposed optimization method for designing large reflectarrays with complexly shaped patterns is reliable and efficient.

Key words: Reflectarray; Dual-polarization; Shaped beam; Phase-only synthesis
https://doi.org/10.1631/FITEE.1900496 **CLC number:** TN828.5

1 Introduction

As a bridge between a satellite and the Earth station, a satellite antenna is a key component of the satellite communication system. The services of geosynchronous communication satellites are limited to specific areas on the Earth in many cases; thus, the satellite antennas are required to have shaped patterns that cover the designated service areas. As is well known, the shaped reflector antenna is an important type of space-borne antenna for communication satellites, due to its advantages such as high radiation efficiencies and large operating bandwidths. However, with a complexly curved surface, the shaped reflector needs considerable volume, adding great difficulty to the overall layout of the satellite. The shaped reflector antenna has another drawback. An elaborate and expensive custom molding is required to fabricate the shaped carbon-fiber reflector. This has a great impact on the antenna performance at higher frequencies.

An alternative choice for the shaped-beam antenna is a microstrip reflectarray antenna proposed by Pozar et al. (1999). In the microstrip reflectarray with

‡ Corresponding author

* Project supported by the National Key Research and Development Program of China (No. 2017YFB0202102)

ORCID: Gang ZHAO, https://orcid.org/0000-0001-6449-8926; Yong-chang JIAO, https://orcid.org/0000-0001-7936-7355

a feed, the reflective surface is a flat quasi-periodic array with many conducting elements printed on a grounded dielectric substrate. Scattering properties of the individual microstrip elements are controlled, progressive reflection phase shifts across the aperture are designed, and then a special wavefront is produced. Reflectarray antennas are the best choice to replace the shaped reflector antennas in the future, thanks to their advantages such as flat structure, low cost, easy deployment, and flexibly shaped patterns.

Although the reflectarray antenna has many advantages, its main shortcoming is that its operating band is relatively narrow, compared with the reflector antenna. Its narrow band characteristic is caused mainly by two factors. One is the inherently narrow bandwidths of the microstrip elements, which greatly affect the operating bands of small reflectarrays. The other is the differential spatial phase delays, which are dominant for large reflectarrays. Many wideband elements, such as sub-wavelength elements (Pozar, 2007), multi-resonant elements (Chaharmir and Shaker, 2008), and rotated elements (Yu et al., 2009), have been proposed to address the first issue. To overcome the second difficulty, Chaharmir et al. (2009) proposed an optimization method to solve the frequency dispersion problem of the large reflectarray.

As is known, dual-polarization antennas in satellite applications should achieve high isolation between two polarizations, which is difficult to realize by conventional reflectors, except dual-grid reflectors. Due to their drawbacks, such as high cost and large volume, dual-grid reflectors are limited in satellite applications. Because the element's orthogonal dimensions can be independently adjusted for different polarizations, reflectarrays can be designed to produce shaped beams with two polarizations (Encinar et al., 2006).

By controlling the reflect phases of the elements, radiation patterns of the microstrip reflectarray are shaped. This process is accomplished by adjusting the dimensions of the elements. Although great progress has been made in computer technology and computational electromagnetic methods, the computational cost for optimizing all the dimensions based on full-wave analyses is still unacceptable for large microstrip reflectarrays. To attain the design goal, it is necessary to propose novel optimal design methods for large microstrip reflectarrays with shaped beams. For medium-size microstrip reflectarrays with shaped beams, Encinar and Zornoza (2004) made important contributions. Scattering analyses of the reflectarray elements and optimization of the array aperture phase distribution were carried out independently, greatly improving the design efficiency and making the design of large microstrip reflectarrays with shaped beams possible. The specific design process is as follows. First, the phase-only syntheses are carried out to obtain the phase distributions of the reflective surface that meet the shaped-beam requirements. Second, the spectral domain method of moments is used to analyze the scattering characteristic of each element, and the element dimensions are optimized to make the reflection phases of each element close to the target phases. Several shaped-beam reflectarrays were designed using the above method (Arrebola et al., 2008; Encinar et al., 2011; Carrasco et al., 2013; Prado et al., 2017). A direct optimization technique based on the gradient minimax algorithm was used to design shaped-beam reflectarrays (Zhou et al., 2013, 2014, 2015). A lookup table of scattering parameters is established to speed up the optimization process. Unfortunately, as the variable number of the elements increases, the time required for generating the table increases as well. In addition, because the interpolation is used, the scattering parameters of the element can hardly be calculated accurately. Recently, a shaped-beam reflectarray was realized using a nonuniform frequency selective surface (FSS) backed element to control both the amplitude and phase (Wu et al., 2018). However, its radiation efficiencies decrease inevitably.

In this paper, a broadband dual-polarized shaped-beam large reflectarray with China-coverage patterns is designed. Due to the complexly shaped areas and high gain requirement, the reflectarray should be large enough. Its aperture size is more than 2 m, and it includes totally 25 000 elements. To the best of our knowledge, such large reflectarrays with complexly shaped patterns have not yet been designed. For very large reflectarrays, there are two serious problems. One is that the spatial phase delay differences (PDPs) in the operating band increase rapidly, as the aperture size of the reflectarray increases. The other is that the optimization of the huge number of reflectarray elements for China-coverage

patterns is a tremendous challenge. To solve these problems, we adopt the following design procedure. First, a three-layer dual-polarization rectangular patch element is addressed. The spectral domain method of moments is used to analyze the reflective coefficients of the element. By optimizing the dimensions of each element, the spatial PDPs in the operating band can be compensated for. Then, the intersection approach is used to determine the phase distributions of the reflective surface, with which the China-coverage shaped patterns are realized by the reflectarray. To ensure convergence of the intersection approach, a new simple method for producing the initial solution is proposed. To reduce the spatial PDPs in the operating band, a new optimization model for each element is established, and the regular polyhedron method is used to solve the model. By repeating the optimization process many times, optimal dimensions of all the elements are determined. Thus, the large microstrip reflectarray can radiate dual-polarization shaped patterns for China coverage in the dual Ku band. To validate the design paradigm, an 87×87-element dual-frequency dual-polarization microstrip reflectarray with shaped patterns is designed and fabricated. The measurement results agree reasonably with the simulation ones. Finally, a 25 305-element broadband microstrip reflectarray is designed successfully. Simulation results indicate that the microstrip reflectarray radiates dual-polarization shaped patterns for China coverage in the dual Ku band, and a very complicated design goal is achieved.

2 Element design

The geometry of the reflectarray element (Fig. 1) is the same as that of the element used in Encinar et al. (2006). The element consists of three identical substrates, and three rectangular patches with sizes $a_1 \times b_1$, $a_2 \times b_2$, and $a_3 \times b_3$ are etched on the three substrates, respectively. The element periods are $d_x=d_y=14$ mm. Parameters a_1, a_2, and a_3 are assumed to satisfy $a_3=a_1\times0.7$ and $a_2=a_1\times0.9$. Parameters b_1, b_2, and b_3 follow the same relations. By adjusting patch dimension a_1 or b_1, the phase shifts for two polarizations can be expected to meet the requirements. Suppose that $a_1=b_1$. When the patch sizes are varied, the phase-shift curves at different frequencies are presented in Fig. 2, and the difference between reflective phases at extreme frequencies are as provided in Fig. 3. As shown in Figs. 2 and 3, the phase-shift range of the element is larger than 700°, and the maximum phase difference between the upper and lower frequencies is close to 250°. Furthermore, when a_1 ranges from 9.0 mm to 12.5 mm, the phase-shift range is more than 360°, and the phase difference is more than 100°. For the general case, if parameters a_1, a_2, a_3, b_1, b_2, and b_3 are adjusted freely in reasonable ranges, the spatial PDP of the microstrip reflectarray will be compensated for to a large extent, and then the broadband dual-polarization shaped patterns of the reflectarray may be realized.

As is known, dielectric losses exist objectively in the substrates. This kind of loss should be fully taken into account when the reflectarray formed by the element is analyzed. Fig. 4 presents the reflection amplitudes of the element at different frequencies. As shown in Figs. 3 and 4, the largest reflection losses occur in the region close to the largest phase

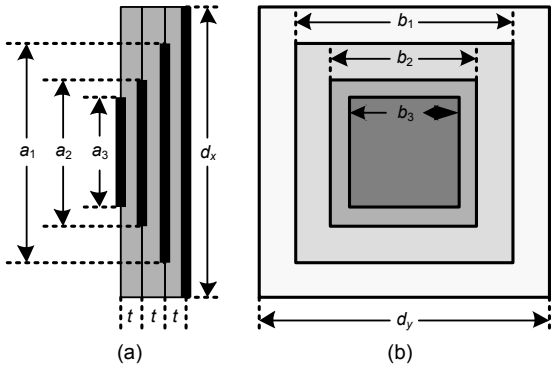

Fig. 1 Geometry of the reflectarray element: (a) side view; (b) top view

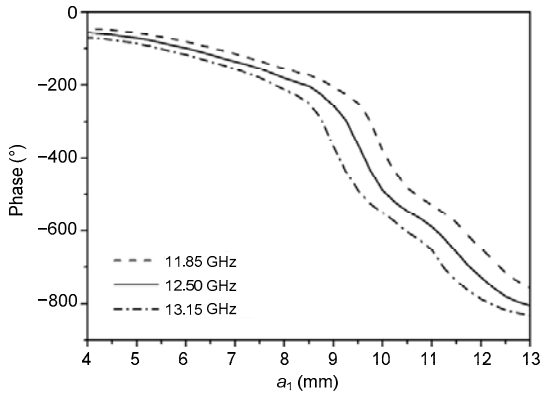

Fig. 2 Reflective phase shifts of the element versus parameter a_1 at three frequencies

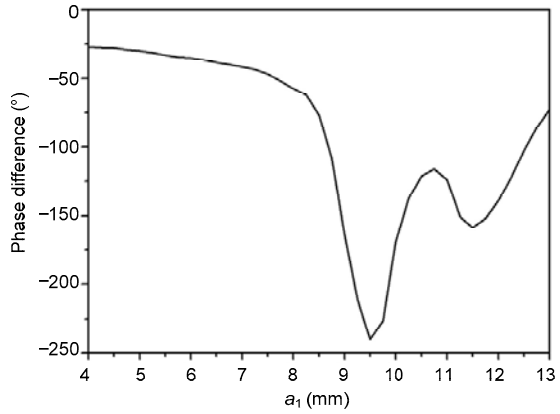

Fig. 3 Difference between phase shifts of the element at upper and lower frequencies versus parameter a_1

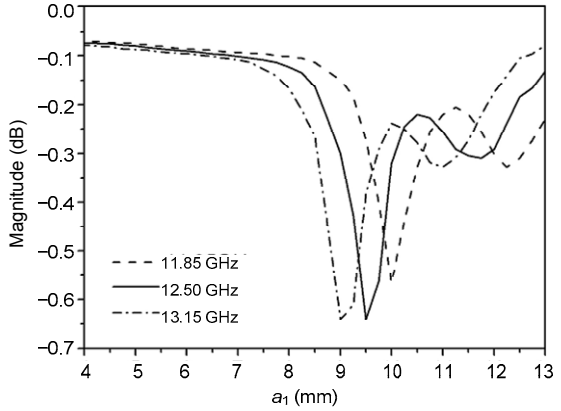

Fig. 4 Reflective magnitudes of the element versus parameter a_1 at three frequencies

difference. The phase adjustment ability and the losses of the element should be taken into account simultaneously, when the element dimensions are determined. Fig. 4 indicates that the minimum reflection amplitude of the element is −0.64 dB, and the element losses are acceptable. Therefore, the three-layer rectangular patch element meets the phase shift requirements in the operating band. It can be used to design the large wideband dual-polarization shaped-beam microstrip reflectarray for China coverage.

3 Synthesis of the shaped-beam reflectarray at a single frequency

3.1 Feed for the reflectarray

As a space-fed array, the reflectarray radiates energy from the elements, illuminated by the feed. Thus, the radiation characteristics of the feed are important for the reflectarray. Due to its advantages, such as high design degree of freedom, flexible radiation patterns, and stable phase center, the corrugated horn is most commonly used as the feed for reflector antennas. Here, the corrugated horn is chosen as the feed for the reflectarray, and its radiation field can be expressed approximately as (Rahmat-Samii et al., 1981)

$$\begin{aligned}\boldsymbol{E}(\theta,\phi)=&\frac{\mathrm{e}^{-\mathrm{j}kr}}{r}\boldsymbol{\theta}U_{\mathrm{E}}(\theta)(c\mathrm{e}^{\mathrm{j}\delta}\cos\varphi+d\sin\varphi)\\&+\boldsymbol{\varphi}U_{\mathrm{H}}(\theta)(d\cos\varphi-c\mathrm{e}^{\mathrm{j}\delta}\sin\varphi),\end{aligned}\tag{1}$$

where r is the distance between the field point and the feed, $U_{\mathrm{E}}(\theta)$ and $U_{\mathrm{H}}(\theta)$ are the E-plane and H-plane patterns of the feed, respectively, denoted by

$$U_{\mathrm{E}}(\theta)=\cos^m\theta,\tag{2}$$

$$U_{\mathrm{H}}(\theta)=\cos^n\theta,\tag{3}$$

where m and n are real numbers, and their specific values are determined by the edge taper levels of the reflectarray. In Eq. (1), the feed polarizations are determined by variables c, d, and δ. Table 1 provides four feed polarizations with different c, d, and δ values.

Table 1 Definition of the feed polarizations

Feed polarization	c	d	δ
x-polarization	1	0	0°
y-polarization	0	1	0°
RHCP	$1/\sqrt{2}$	$1/\sqrt{2}$	90°
LHCP	$1/\sqrt{2}$	$1/\sqrt{2}$	−90°

RHCP: right-hand circular polarization; LHCP: left-hand circular polarization

3.2 Far fields of the reflectarray

According to the diffraction theory, the far-field radiation characteristics of the aperture antenna can be obtained from the tangential components of its aperture field (Clark and Brown, 1980). The far-field electric vector of the reflectarray is expressed as

$$\begin{aligned}\boldsymbol{E}(\theta,\varphi)=\mathrm{j}k\big[&(\boldsymbol{\theta}\cos\varphi-\boldsymbol{\varphi}\sin\varphi\cos\theta)\tilde{E}_{rx}\\&+(\boldsymbol{\theta}\sin\varphi+\boldsymbol{\varphi}\cos\varphi\cos\theta)\tilde{E}_{ry}\big]\frac{\mathrm{e}^{-\mathrm{j}kr}}{2\pi r},\end{aligned}\tag{4}$$

where $\tilde{E}_{rx}$ and $\tilde{E}_{ry}$ are the spectral functions of the tangential components of the aperture field, denoted by

$$\tilde{E}_{rx}(\theta,\varphi)=\iint_{\text{Rarray}} E_x(x,y)\mathrm{e}^{\mathrm{j}(k_x x+k_y y)}\mathrm{d}x\mathrm{d}y, \tag{5a}$$

$$\tilde{E}_{ry}(\theta,\varphi)=\iint_{\text{Rarray}} E_y(x,y)\mathrm{e}^{\mathrm{j}(k_x x+k_y y)}\mathrm{d}x\mathrm{d}y. \tag{5b}$$

$\tilde{E}_{rx}$ in Eq. (5a) is calculated by

$$\begin{aligned}\tilde{E}_{rx}(p,q)=d_x d_y&\operatorname{sinc}\left(\frac{k_x d_x}{2}\right)\operatorname{sinc}\left(\frac{k_y d_y}{2}\right)\\&\cdot\exp\left(-\frac{1}{2}\mathrm{j}(k_x(N_x-1)d_x+k_y(N_y-1)d_y)\right)\\&\cdot\sum_{m=0}^{N_x-1}\sum_{n=1}^{N_y-1}\left[A_x(m,n)\exp(\mathrm{j}\phi_x(m,n))\right.\\&\left.\cdot\exp\left(\mathrm{j}\frac{2mp\pi}{N_x}\right)\exp\left(\mathrm{j}\frac{2nq\pi}{N_y}\right)\right],\end{aligned} \tag{6}$$

where p=0, 1, …, N_x−1, q=0, 1, …, N_y−1, and $A_x(m, n)$ and $\phi_x(m, n)$ are the amplitude and phase of the $(m, n)^{\text{th}}$ element, respectively. The two-dimensional (2D) inverse discrete fast Fourier transform (DFFT) can be used to calculate the double summation in Eq. (6) conveniently. Thus, the spectral functions and the radiation patterns can be obtained efficiently. Moreover, DFFT and inverse DFFT can be used to establish a one-to-one relationship between the aperture field distribution and the far field, which lays a foundation for optimizing the reflectarray.

3.3 Shaped-beam synthesis of the microstrip reflectarray by the intersection approach

When the geometry of the microstrip reflectarray is fixed, the reflective amplitude of the passive reflectarray element is determined by the feed pattern, which is close to that of the total reflection. Our design goal is that the specified shaped beams are realized by the reflectarray. To achieve this goal, reflection phases of all the elements in the reflectarray should be optimized first, known as phase-only synthesis. In recent years, some evolutionary algorithms, such as the genetic algorithm, particle swarm optimization algorithm, and differential evolution algorithm, have been applied in antenna designs (Rahmat-Samii and Michielssen, 1999; Robinson and Rahmat-Samii, 2004; Zhang et al., 2009). However, due to their excessive computation, these evolutionary algorithms are seldom used to optimize very large reflectarrays with a huge number of elements. It is necessary to propose a method to optimize the reflection phases of all the elements of large reflectarrays, especially reflectarrays with more than 5000 elements.

As shown in Section 3.2, there is a one-to-one relationship between the aperture field distribution and the far field, which is established by DFFT and inverse DFFT. Therefore, the intersection approach based on the alternating projection (Bucci and Franceschetti, 1990) can be used to optimize the reflection phases of all the elements of large reflectarrays with shaped beams (Encinar and Zornoza, 2004).

In the intersection approach, there are two sets, i.e., set M, in which the radiation patterns meet the mask requirements, and set B, which consists of the excitation coefficients realized by the reflectarray. Specifically, set M is defined as

$$M=\left\{F: M_{\mathrm{L}}(u,v)\le\left|F(u,v)\right|\le M_{\mathrm{U}}(u,v)\right\}, \tag{7}$$

where (u, v) are the angular coordinates, $F(u, v)$ is the far-field radiation pattern of the reflectarray, $M_{\mathrm{L}}(u, v)$ and $M_{\mathrm{U}}(u, v)$ are the lower and upper bounds for the radiation patterns, respectively. Set B is defined as

$$B=\left\{J_{mn}: J_{\mathrm{L}}(m,n)\le\left|J(m,n)\right|\le J_{\mathrm{U}}(m,n)\right\}, \tag{8}$$

where (m, n) represents the $(m, n)^{\text{th}}$ element in the reflectarray, $J(m, n)$ is the excitation coefficient of the $(m, n)^{\text{th}}$ element, and $J_{\mathrm{L}}(m, n)$ and $J_{\mathrm{U}}(m, n)$ are the lower and upper amplitude bounds for the $(m, n)^{\text{th}}$ element, respectively. The alternating projection process can be depicted as

$$\begin{aligned}F(u,v)_{n+1}&=\mathrm{IDFFT}\{P_B\{\mathrm{DFFT}[P_M F(u,v)_n]\}\}\\&=\mathrm{IDFFT}\{P_B J'(m,n)_n\},\end{aligned} \tag{9}$$

where P_M and P_B are the projection operators on sets M and B, respectively. According to Eq. (7), projection operator P_M is expressed as

$$P_M F(u,v)=\begin{cases} M_{\mathrm{U}}(u,v)\dfrac{F(u,v)}{|F(u,v)|}, & |F(u,v)|>M_{\mathrm{U}}(u,v), \\ F(u,v), & M_{\mathrm{L}}(u,v)\le|F(u,v)|\le M_{\mathrm{U}}(u,v), \\ M_{\mathrm{L}}(u,v)\dfrac{F(u,v)}{|F(u,v)|}, & |F(u,v)|<M_{\mathrm{L}}(u,v), \end{cases} \tag{10}$$

where the real radiation pattern of the reflectarray is corrected, making $F(u, v)$ belong to set M. Projection operator P_B is defined as

$$P_B J(m,n)=\begin{cases} J_{\mathrm{U}}(m,n)\dfrac{J(m,n)}{|J(m,n)|}, & J(m,n)>J_{\mathrm{U}}(m,n), \\ J(m,n), & J_{\mathrm{L}}(m,n)\le|J(m,n)|\le J_{\mathrm{U}}(m,n), \\ J_{\mathrm{L}}(m,n)\dfrac{J(m,n)}{|J(m,n)|}, & |J(m,n)|<J_{\mathrm{L}}(m,n), \end{cases} \tag{11}$$

where the excitation coefficient $J(m, n)$ is projected onto set B. By iteratively projecting between sets B and M, the intersection approach can be used to obtain their intersection or a solution in set B, which approaches set M as close as possible.

Because the intersection approach is a local optimization method, a reasonable initial solution is important for its convergence. Generally, a method for producing the initial solution is described as follows. First, an alternative shaped reflector antenna with the specified shaped beams is designed. The shaped reflector antenna has the same geometry as the microstrip reflectarray, except that the shaped reflector is replaced by the microstrip patch array. Then, the aperture phase distribution of the shaped reflector (Pozar et al., 1999) is chosen as the initial solution of the intersection approach. This method is inconvenient, because it is difficult to design the shaped reflector. To overcome the difficulty of the method, we propose a new simple method for producing the initial solution. First, a microstrip reflectarray with pencil beams is designed. Then, as shown in Fig. 5, by properly moving the feed toward the reflectarray, a suitable out-of-phase distribution of the reflectarray is obtained, which is chosen as the initial phase distribution.

As an example, an elliptical microstrip reflectarray with a square-shaped beam is designed. The out-of-focus initial solution and the optimization results are also demonstrated. The elliptical microstrip reflectarray with size 2.002 m×1.918 m is placed in the *xoy* plane, and designed to radiate a square-shaped beam in the direction with θ=15°. The element size is defined as 14 mm×14 mm. The reflectarray with 75 columns and 71 rows has a total of 15 437 elements. The coordinates of the feed phase center are x_f=−0.6 m, y_f=0 m, and z_f=1.1 m. The operating frequency is set to be 12.50 GHz. First, a 15 437-element microstrip reflectarray with pencil beams is designed, and its peak gain is 46 dBi in the direction with θ=15°. In this case, phases of the reflected field and the incident field for the $(m, n)^{\mathrm{th}}$ element are denoted by $\varphi_{\mathrm{r}}(m, n)$ and $\varphi_{\mathrm{i}}(m, n)$, respectively, and the element phase shift is represented as $\varphi_{\mathrm{s}}(m, n)$. Obviously,

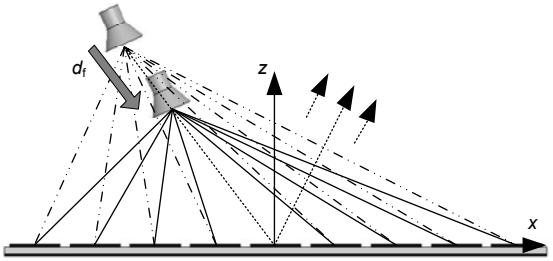

Fig. 5 A new simple method for producing the out-of-focus initial solution

$$\varphi_{\mathrm{r}}(m,n)=\varphi_{\mathrm{i}}(m,n)+\varphi_{\mathrm{s}}(m,n). \tag{12}$$

If $\varphi_{\mathrm{r}}(m, n)$ is chosen as the initial phase solution directly, the intersection approach converges to a local minimum with narrow hollows inside the shaped beam.

Then, as shown in Fig. 5, the feed is moved toward the reflectarray, and the phase of the incident field changes from $\varphi_{\mathrm{i}}(m, n)$ to $\varphi_{\mathrm{i}}'(m, n)$. When the element phase shifts are fixed, the phase of the reflected field is expressed as

$$\varphi_{\mathrm{r}}'(m,n)=\varphi_{\mathrm{i}}'(m,n)+\varphi_{\mathrm{s}}(m,n), \tag{13}$$

where $\varphi_{\mathrm{r}}'(m, n)$ is the out-of-focus phase of the $(m, n)^{\mathrm{th}}$ element. Using the new method, $\varphi_{\mathrm{r}}'(m, n)$ is chosen as the initial phase solution for the $(m, n)^{\mathrm{th}}$ element. The movement distance of the feed is defined as d_f. When d_f equals 5λ at 12.50 GHz, the contour pattern of the out-of-focus beam is shown in

Fig. 6a. It can be seen that the peak gain is less than that of the pencil beam, and the beamwidth increases.

Taking $\varphi_r'(m, n)$ as the initial phase solution for the $(m, n)^{th}$ element, the intersection approach with unchanged edge illumination is carried out, and the optimal contour beam is shown in Fig. 6b. There are no hollows in the shaped region. In summary, using the new method to produce the initial phase solution, the intersection approach converges to a good solution without hollows, provided that sidelobes of the pattern corresponding to the initial phase solution do not appear in the shaped region.

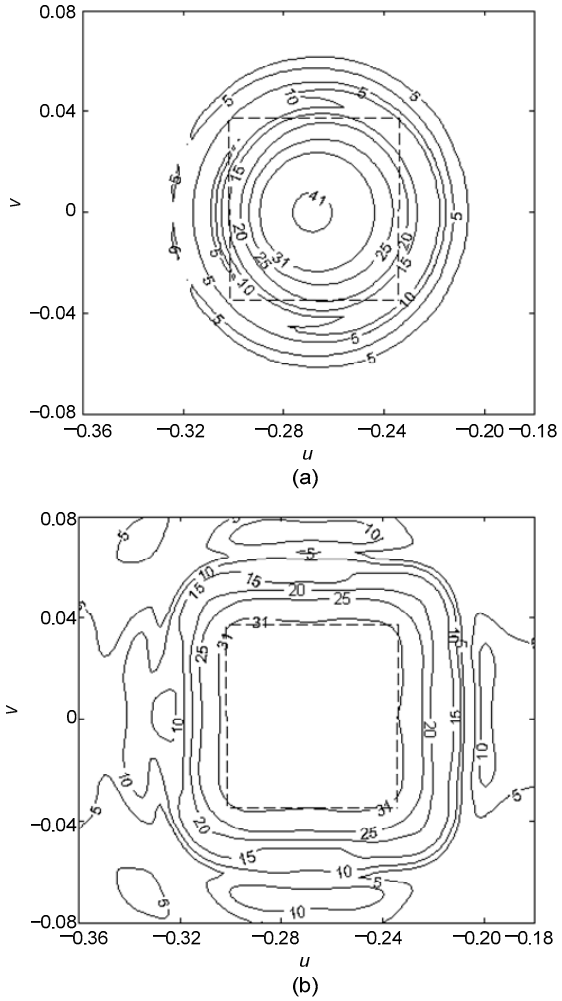

Fig. 6 Contour patterns of the reflectarray: (a) out-of-focus beam; (b) optimized beam

3.4 Design of the medium-size reflectarray and its experimental verification

To validate the synthesis method, a medium-size dual-polarization shaped-beam microstrip reflectarray is designed, fabricated, and measured. The reflectarray radiates horizontally and vertically polarized waves in the 12.25–12.75 GHz band and the 14.00–14.50 GHz band, respectively. Two corrugated horns are used as two feeds of the reflectarray for two polarizations. To realize dual-polarized shaped beams, a two-layer rectangular microstrip patch element is adopted for the reflectarray, similar to the element in Fig. 1. The array period is 14 mm. Parameters a_1, a_2, b_1, and b_2 are assumed to satisfy two equations $a_2=a_1\times0.7$ and $b_2=b_1\times0.7$. The reflectarray with 87 columns and 87 rows has totally 7569 elements, and its aperture is 1.218 m×1.218 m. Because the spatial PDPs of the medium-size reflectarray in two operating bands are not so large, the dimensions of each element are determined by matching its real reflection phases calculated by the spectral-domain method of moments to its desired phases at only two central frequencies. Photographs of the fabricated reflectarray are shown in Fig. 7.

Patterns of the reflectarray are measured using a near-field measurement system. Simulated and measured patterns of the reflectarray are presented in Figs. 8 and 9, respectively. It can be seen that the measurement results agree reasonably with the simulation ones. Their coincidence degree in the 12.25–12.75 GHz band is better than that in the 14.00–14.50 GHz band. Some discrepancies between the measured and simulated patterns still exist. The main reasons for these discrepancies can be summarized as follows: (1) Large reflectarrays are composed of several small sub-arrays. Each layer is fabricated separately, and these two layers are bonded by hand. The rectangular patches in two layers cannot be aligned strictly and the largest misalignment is larger than one array period, which heavily impacts the phase shifts of the elements, causing phase-shift deterioration. (2) Because the one-layer substrate is a multi-layer sandwich composite structure made of Kevlar and honeycomb materials, its uniformity is hardly guaranteed, leading to phase shift deterioration for each element. (3) As shown in Fig. 7b, the array plane is separated from the metallic support plane, and the spatial path delays of the entire reflectarray are changed. Due to the shorter wavelength, the coincidence degree between simulated and measured patterns in the 14.00–14.50 GHz band is worse than that in the 12.25–12.75 GHz band. Although there

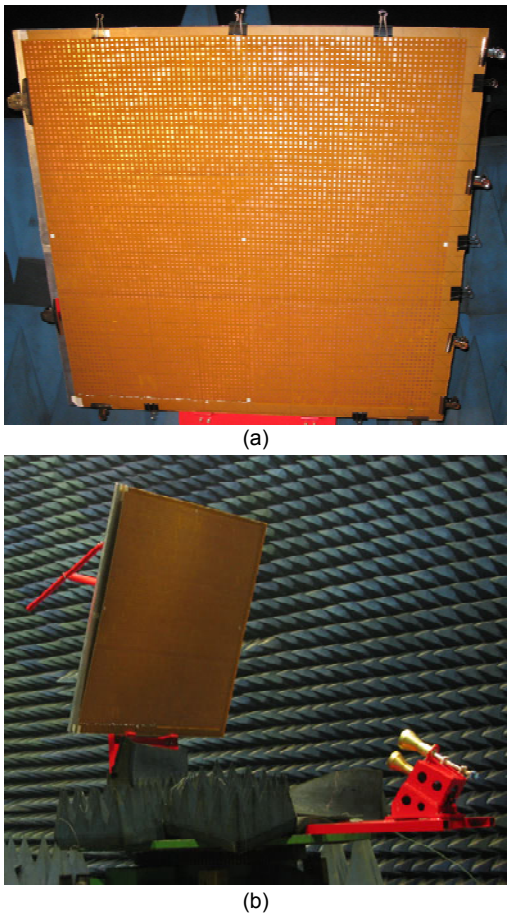

(a)

(b)

Fig. 7 Photographs of the medium-size reflectarray (a) and its measurement (b)

are some discrepancies between the measurement and simulation results, the efficiency of the synthesis method is still validated.

4 Design of the large broadband dual-polarization shaped-beam reflectarray with China coverage

4.1 Offset-fed configuration design

The bandwidth of the large reflectarray is drastically limited by the great spatial PDPs between the edge elements and the center element in the operating band. To broaden its bandwidth, it is necessary to compensate for PDPs. Because PDPs depend solely on the locations of the elements and the position of the feed, an optimal position of the feed exists, and PDPs can be reduced. The reduced PDPs are compensated for easily by the element dimensions.

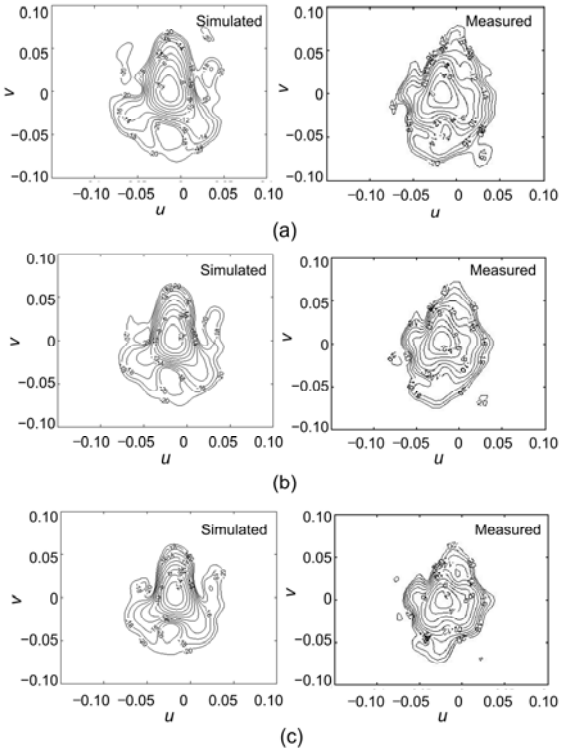

Fig. 8 H-polarization radiation patterns of the medium-size reflectarray at central and extreme frequencies: (a) 12.25 GHz; (b) 12.50 GHz; (c) 12.75 GHz

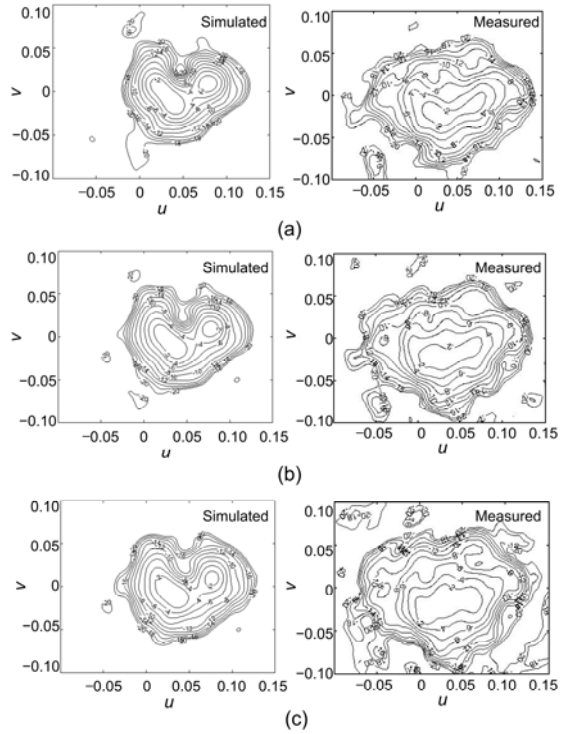

Fig. 9 V-polarization radiation patterns of the medium-size reflectarray at central and extreme frequencies: (a) 14.00 GHz; (b) 14.25 GHz; (c) 14.50 GHz

For the prime-focus reflectarray, the feed is located above the aperture center. When the main beam of the reflectarray points to the boresight direction, the distribution of PDPs over the reflectarray aperture is symmetrical, and the maximum PDP is minimized. Therefore, all the positions on the boresight axis are optimal feed positions. However, the reflected waves of the prime-focus reflectarray are blocked by the feed. This may negatively affect the impedance matching of the feed, and reduce the radiation efficiencies of the reflectarray. Usually, an offset-fed configuration is suggested to avoid the feed blockage.

A diagram of the offset-fed configuration is shown in Fig. 10. Without loss of generality, we assume that the phase center of the offset feed is located at the *xoz* plane. Its coordinates are defined as (x_f, 0, z_f), and the main beam of the reflectarray points to the θ direction. In this case, the reflectarray configuration is dissymmetrical, and the following geometric relationship should be satisfied to minimize the maximum PDP:

$$d_1^i = d_2^i + d^r, \tag{14}$$

which can be expressed as

$$z_f^2 = x_f^2 \cot^2\theta - 0.25D^2 \cos^2\theta, \tag{15}$$

where D represents the aperture dimension of the reflectarray. Eq. (15) governs the coordinate relations that correspond to the optimal feed position.

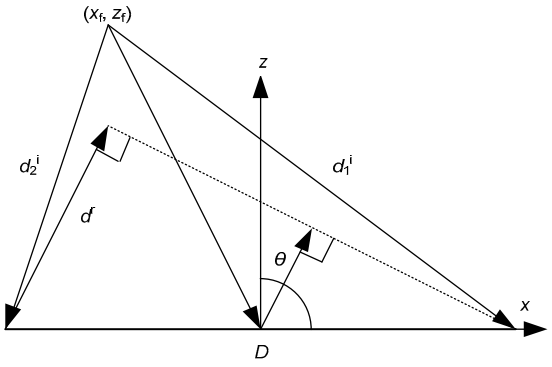

Fig. 10 Diagram of the offset-fed configuration

Fig. 11 presents several curves of the coordinate relations of the optimal feed position with different aperture dimensions and beam scan angles. As shown in Fig. 11, offset-fed reflectarrays with different aperture dimensions and beam scan angles have different optimal feed positions. For a given offset-fed reflectarray, we can find the optimal feed position on the corresponding curve by considering the best trade-off among some factors such as feed blockage, radiation efficiency, and the F/D ratio.

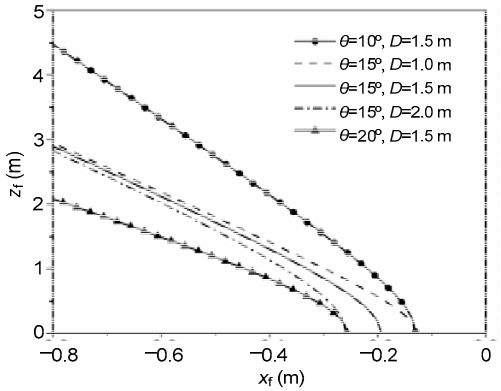

Fig. 11 Curves of the optimal feed positions with different aperture sizes and beam scanning angles

4.2 Element dimension optimization for the large broadband reflectarray

As discussed in Section 3.2, using the intersection approach, the reflection phase of each element required for the reflectarray with the China-coverage pattern at the central frequency can be obtained. Because the optical path is dispersed by the frequencies, the desired phase shift of each element at the extreme frequencies can also be obtained easily by adding or subtracting an offset-path phase from its phase at the central frequency. Once the desired phase shifts of each element at some sample frequencies in the operating band are obtained, the dimensions of each element can be determined. This is realized by combining a full-wave electromagnetic analysis technique with an optimization method. Under the Floquet periodic boundary conditions, a full-wave spectral-domain method of moments (Vacchione, 1990) is used to analyze the scattering characteristic of each element with real incidence angle and polarization. Our design goal is to find the simultaneously optimal dimensions of each element in two orthogonal directions such that its real reflective phases approach the desired phase shifts at some sample frequencies in the operating band as close as possible. To achieve this goal, we establish the following optimization model for the $(m, n)^{th}$ element:

$$\begin{aligned}&\text{minimize} \quad e(\boldsymbol{v}^{(m,n)})\\&\text{subject to} \quad a_i^{\mathrm{L}} \le a_i \le a_i^{\mathrm{U}}, b_i^{\mathrm{L}} \le b_i \le b_i^{\mathrm{U}},\ i=1,2,3,\\&\qquad \boldsymbol{v}^{(m,n)} = (a_1,a_2,a_3,b_1,b_2,b_3)^{\mathrm{T}},\end{aligned} \tag{16}$$

where

$$\begin{aligned}e(\boldsymbol{v}^{(m,n)}) = \sum_{i=1}^{N_{\mathrm{f}}} \Big[&\left|\varphi_{\mathrm{a}}^{x}(f_i,\boldsymbol{v}^{(m,n)}) - \varphi_{\mathrm{r}}^{x}(f_i)\right| \\ &+ \left|\varphi_{\mathrm{a}}^{y}(f_i,\boldsymbol{v}^{(m,n)}) - \varphi_{\mathrm{r}}^{y}(f_i)\right| \Big].\end{aligned} \tag{17}$$

Herein a_i^{L}, b_i^{L} and a_i^{U}, b_i^{U} are the lower and upper bounds for parameters a and b of the $(m, n)^{\mathrm{th}}$ element, respectively; f_i is the sample frequency in the operating band (i=1, 2, …, N_{f}); $\varphi_{\mathrm{a}}^{x}(f_i,\boldsymbol{v}^{(m,n)})$ and $\varphi_{\mathrm{a}}^{y}(f_i,\boldsymbol{v}^{(m,n)})$ are the real phase shifts of the $(m, n)^{\mathrm{th}}$ element at frequency f_i corresponding to its dimension vector $\boldsymbol{v}^{(m,n)}$ for x- and y-polarization, respectively; $\varphi_{\mathrm{r}}^{x}(f_i)$ and $\varphi_{\mathrm{r}}^{y}(f_i)$ are the desired phase shifts of the $(m, n)^{\mathrm{th}}$ element at frequency f_i for x- and y-polarization, respectively. The optimization problem (16) is solved by the regular polyhedron method (Jiao et al., 1993). Because the regular polyhedron method is a local direct optimization method, a suitable initial point should be provided in advance. When four equations a_3=a_1×0.7, a_2=a_1×0.9, b_3=b_1×0.7, and b_2=b_1×0.9 are satisfied, the dimensions of the $(m, n)^{\mathrm{th}}$ element, i.e., $\left(a_1^0,a_2^0,a_3^0,b_1^0,b_2^0,b_3^0\right)$, can be determined by its desired phase shift at the central frequency, chosen to form an initial point $\boldsymbol{x}_0^{(m,n)} = \left(a_1^0,a_2^0,a_3^0,b_1^0,b_2^0,b_3^0\right)^{\mathrm{T}}$. With the initial point $\boldsymbol{x}_0^{(m,n)}$, the regular polyhedron method is used to solve problem (16), and the optimal dimension vector $\boldsymbol{x}_*^{(m,n)}$ is obtained for the $(m, n)^{\mathrm{th}}$ element. By repeating the aforementioned optimization process many times, we can find the dimensions of all the elements in the reflectarray. Thus, the element dimension optimization for the large broadband reflectarray with shaped-beam patterns is completed.

4.3 Design of the large dual-polarization reflectarray with China-coverage patterns

The large dual-polarization reflectarray is required to meet the gain specifications over the China continent coverage. The desired antenna gains in some areas in eastern China and other areas in China are larger than 33 dBi and 28 dBi, respectively. The required cross-polarization levels in these shaped areas are less than −30 dB. The reflectarray is required to operate in the 12.25–12.75 GHz and 14.00–14.50 GHz bands with horizontal and vertical polarizations, respectively.

To meet the gain requirements, a three-layer rectangular microstrip reflectarray with a 2.3 m× 2.2 m elliptical aperture is designed. The configuration of the dual-polarization reflectarray with two feeds is shown in Fig. 12. The reflective surface consists of 185 columns and 175 rows, with a total of 25 305 three-layer rectangular patch elements distributed uniformly in a square grid. To ensure patterns of the reflectarray with no grating lobes, the grid period is chosen as 12.5 mm, which is about 0.6 times the wavelength at 14.25 GHz. Two corrugated horns operating in the 12.25–12.75 GHz and 14.00–14.50 GHz bands are chosen as two feeds for two polarizations, and their radiation patterns are approximated by $\cos^q\theta$, where q is a positive real number. Each horn illuminates the reflectarray edge with −16 dB level, which is a typical value for shaped reflectors.

Using the new simple method, a suitable out-of-focus initial phase distribution is obtained for the large reflectarray with 25 305 elements. Then the intersection approach is used to acquire the desired phase shifts of all the elements for the reflectarray with the China-coverage pattern at some sample frequencies in the operating band.

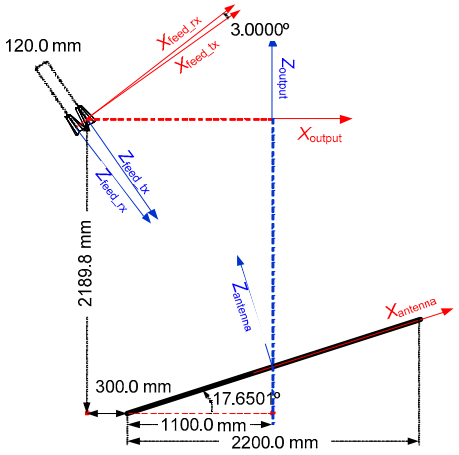

Fig. 12 Configuration of the large dual-frequency dual-polarization reflectarray with China-coverage patterns

In our design, two linearly polarized feeds illuminate the reflectarray, and the directions of their projection fields on the reflective surface are parallel to the two edges of the rectangular patches, respectively. Therefore, the phase shifts for two polarizations can be controlled independently by three lengths of the corresponding patch edges to a large degree. To improve the shaped design results, six parameters of each element in two orthogonal directions are optimized simultaneously by solving problem (16) using the regular polyhedron method. The optimization process is repeated 25 305 times, and the optimal dimensions of all the elements are found. The optimized reflectarray at some sample frequencies are analyzed using the full-wave spectral-domain method of moments, and its radiation patterns are calculated using the inverse DFFT.

For the design of the 25 305-element microstrip reflectarray with China-coverage patterns, if the dimensions of all the elements are optimized at the same time, a nonlinear optimization problem with 151 830 variables should be solved, which is an impossible mission. In this study, the complex optimal design problem is decomposed into 25 305 nonlinear optimization problems with six variables, which can be finished on a common microcomputer.

When the reflectarray is optimized at only the central frequencies 12.50 and 14.25 GHz, the co-polarization gain contour maps at the central and extreme frequencies are plotted in Figs. 13 and 14, respectively. For comparison, the corresponding desired gain contour maps are also depicted in Figs. 13 and 14. Note that the desired gain contour maps (Figs. 13 and 14) in the reflectarray coordinate system are the mirror images of those in the satellite coordinate system. As shown in Figs. 13 and 14, although the patterns of the optimized reflectarray at 12.50 and 14.25 GHz meet the coverage requirements, the patterns at 12.25, 12.75, 14.00, and 14.50 GHz are distorted, with hollows in the coverage areas and higher sidelobes near the main beams. It is necessary to optimize the reflectarray at the central and extreme frequencies in two operating bands. The co-polarization gain contour maps of the optimized reflectarray at these frequencies are plotted in Figs. 15 and 16, where the gain patterns of the reflectarray meet the China-coverage shaped-beam requirements in two operating bands. Similar to the shaped reflector, the patterns of the reflectarray have slight distortion at very few frequencies. This situation occurs at 14.50 GHz. In this case, more than 90% areas of China coverage meet the gain requirements. The reason for this distortion is that PDPs in this band are greater than those in the lower band, and are more difficult to compensate for. The cross-polarization patterns of the reflectarray for two orthogonal polarizations are also calculated, and the cross-polarization levels are below −35 dB in the coverage areas. By optimizing the dimensions of all the elements, the patterns of the large microstrip reflectarray cover the desired China continent in two operating bands. Therefore, we conclude that simultaneous optimization of the reflectarray in two operating bands is very critical and necessary for the large reflectarray with complexly shaped patterns.

In Encinar et al. (2006), a different method was used to optimize the shaped-beam reflectarray in two operating bands. The objective function is defined by the phase shift error at the center frequency and the PDP error with different weight coefficients. It is difficult to choose suitable weight coefficients in advance, because usually these coefficients are selected according to repeated tests or designers' experience. In our opinion, the design method proposed by Encinar et al. (2006) can hardly be used to optimize large reflectarrays with more than 20 000 elements and with complexly shaped patterns. In this study, the objective function is defined by phase shift errors at the central and extreme frequencies without weight coefficients. Therefore, our design method is more reliable, and can be used to optimize very large reflectarrays with complexly shaped patterns.

5 Conclusions

In this paper, a large dual-band dual-polarization reflectarray with China-coverage patterns is designed for satellite communication. First, the three-layer rectangular patch element is addressed. It is suitable for the large dual-polarization reflectarray. Then, DFFT and inverse DFFT are used to establish a one-to-one relationship between the aperture field distribution and the far field, which lays a foundation for optimizing the shaped-beam reflectarray. The intersection approach based on the alternating projection is used to solve the phase-only synthesis

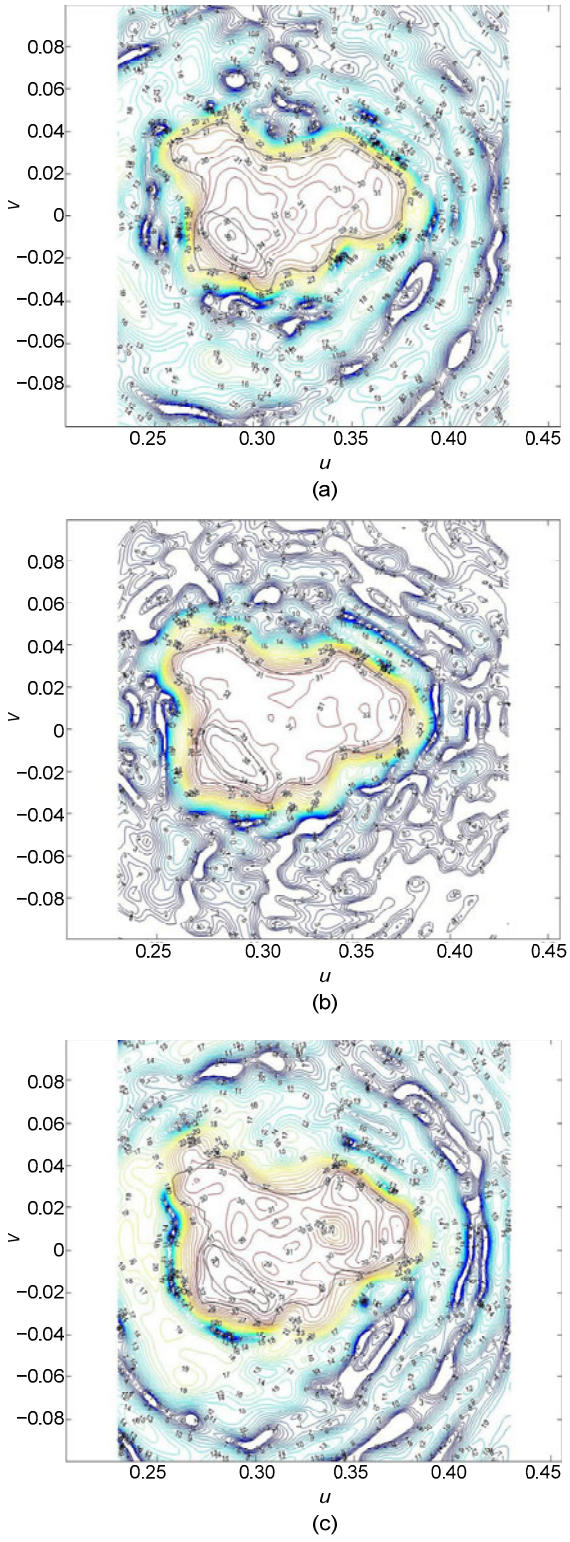

Fig. 13 Radiation patterns at the central and extreme frequencies for the large reflectarray optimized at only two central frequencies: (a) 12.25 GHz; (b) 12.50 GHz; (c) 12.75 GHz

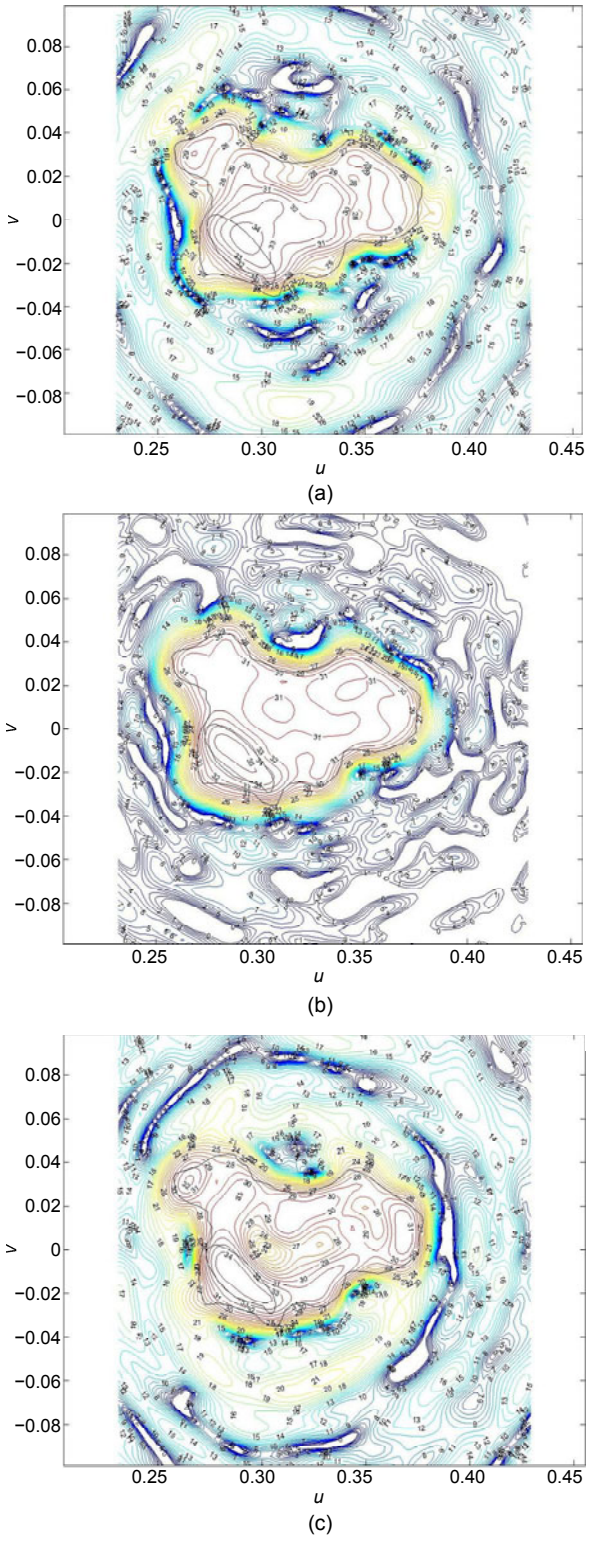

Fig. 14 Radiation patterns at the central and extreme frequencies for the large reflectarray optimized at only two central frequencies: (a) 14.00 GHz; (b) 14.25 GHz; (c) 14.50 GHz

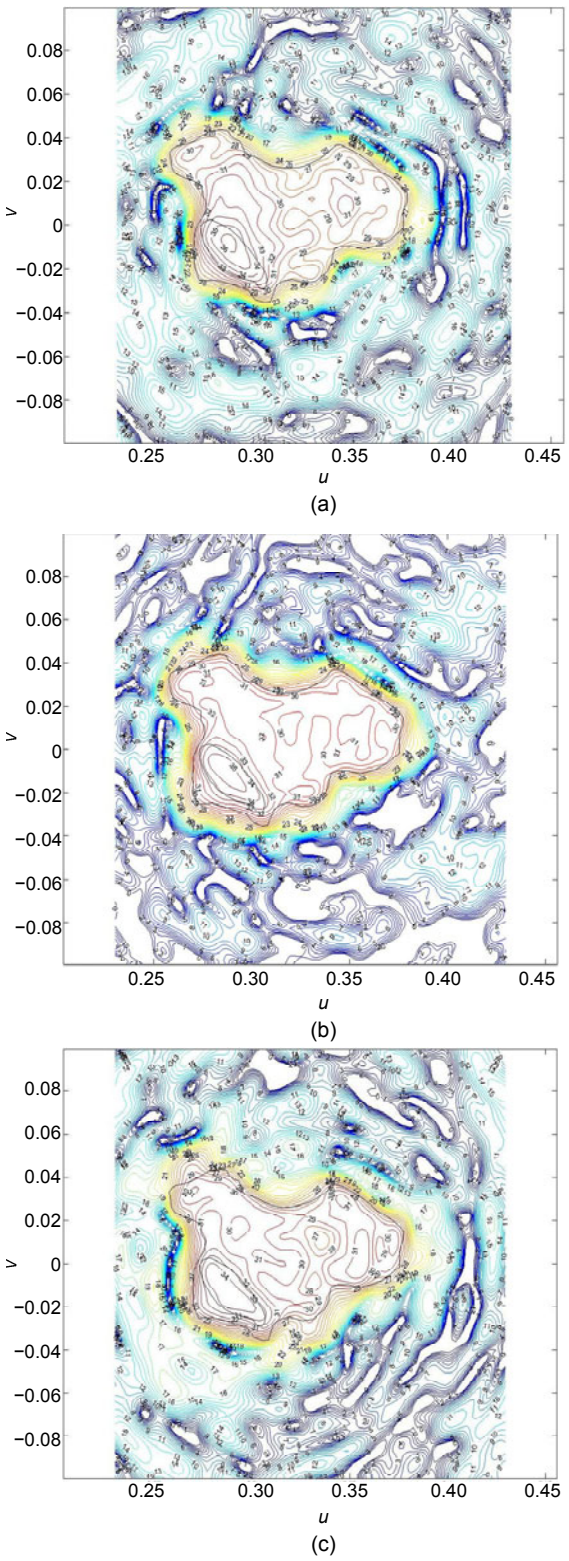

Fig. 15 Radiation patterns at the central and extreme frequencies for the large reflectarray optimized in two operating bands: (a) 12.25 GHz; (b) 12.50 GHz; (c) 12.75 GHz

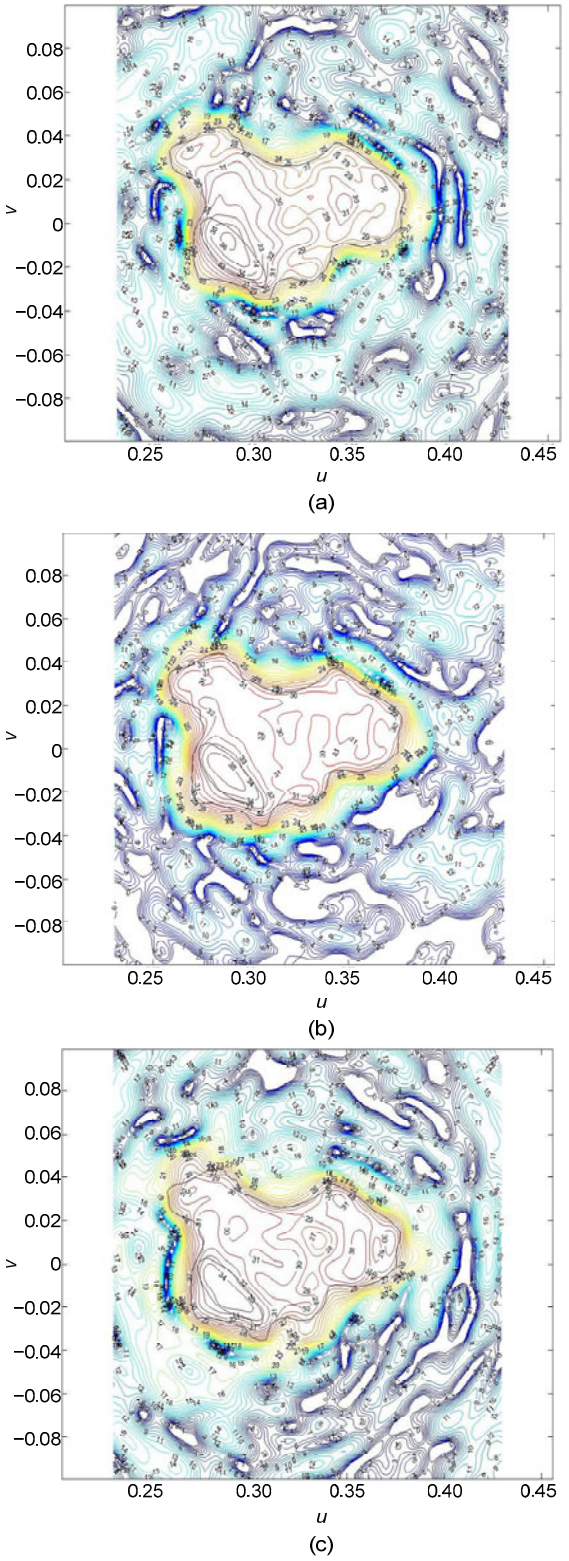

Fig. 16 Radiation patterns at the central and extreme frequencies for the large reflectarray optimized in two operating bands: (a) 14.00 GHz; (b) 14.25 GHz; (c) 14.50 GHz

problem, and a new method for producing a suitable initial solution is proposed to avoid undesired local minima. As a result, the desired reflection phases of all the elements of large reflectarrays with shaped beams are obtained. To validate the design method, a medium-size dual-polarization shaped-beam reflectarray with 7569 elements is designed, fabricated, and measured. The measurement results agree reasonably with the simulation ones. Finally, for the broadband large reflectarray with minimum differential spatial phase delays in the operating band, an approach is presented to determine the optimal position of the feed. A new optimization model is established to find simultaneously optimal dimensions of each element in two orthogonal directions such that its real reflective phases approach the desired phase shifts as close as possible at some sample frequencies in the operating band. The model is solved by the regular polyhedron method. Based on these methods, a dual-band dual-polarization microstrip reflectarray with 25 305 elements is designed to cover the China continent. Simulation results show that the radiation patterns of the reflectarray meet the China-coverage requirements in two operating bands. Our design method can be used to design other very large reflectarrays with complexly shaped patterns.

Contributors

Gang ZHAO designed the research. Gang ZHAO and Guan-tao CHEN processed the data. Gang ZHAO wrote the first draft of the manuscript. Yong-chang JIAO and Guan-tao CHEN helped organize the manuscript. Gang ZHAO and Yong-chang JIAO revised and edited the final version.

Compliance with ethics guidelines

Gang ZHAO, Yong-chang JIAO, and Guan-tao CHEN declare that they have no conflict of interest.

References

Arrebola M, Encinar JA, Barba M, 2008. Multifed printed reflectarray with three simultaneous shaped beams for LMDS central station antenna. *IEEE Trans Antenn Propag*, 56(6):1518-1527. https://doi.org/10.1109/TAP.2008.923360

Bucci O, Franceschetti G, 1990. Intersection approach to array pattern synthesis. *IEE Proc H Microw Antenn Propag*, 137(6):349-357. https://doi.org/10.1049/ip-h-2.1990.0064

Carrasco E, Barba M, Encinar JA, et al., 2013. Design, manufacture and test of a low-cost shaped-beam reflectarray using a single layer of varying-sized printed dipoles. *IEEE Trans Antenn Propag*, 61(6):3077-3085. https://doi.org/10.1109/TAP.2013.2254431

Chaharmir MR, Shaker J, 2008. Broadband reflectarray with combination of cross and rectangle loop elements. *Electron Lett*, 44(11):658-659. https://doi.org/10.1049/el:20080910

Chaharmir MR, Shaker J, Legay H, 2009. Broadband design of a single layer large reflectarray using multi cross loop elements. *IEEE Trans Antenn Propag*, 57(10):3363-3366. https://doi.org/10.1109/TAP.2009.2029600

Clark RH, Brown J, 1980. Diffraction Theory and Antennas. Halsted Press, New York, USA. https://doi.org/10.1016/0029-8018(81)90030-5

Encinar JA, Zornoza JA, 2004. Three-layer printed reflectarrays for contoured beam space applications. *IEEE Trans Antenn Propag*, 52(5):1138-1148. https://doi.org/10.1109/TAP.2004.827506

Encinar JA, Datashvili LS, Zornoza JA, et al., 2006. Dual-polarization dual-coverage reflectarray for space applications. *IEEE Trans Antenn Propag*, 54(10):2827-2837. https://doi.org/10.1109/TAP.2006.882172

Encinar JA, Arrebola M, Fuente LDL, et al., 2011. A transmit-receive reflectarray antenna for direct broadcast satellite applications. *IEEE Trans Antenn Propag*, 59(9):3255-3264. https://doi.org/10.1109/TAP.2011.2161449

Jiao YC, Wei WY, Huang LW, et al., 1993. A new low-side-lobe pattern synthesis technique for conformal arrays. *IEEE Trans Antenn Propag*, 41(6):824-831. https://doi.org/10.1109/8.250466

Pozar DM, 2007. Wideband reflectarrays using artificial impedance surfaces. *Electron Lett*, 43(3):148-149. https://doi.org/10.1049/el:20073560

Pozar DM, Targonski SD, Pokuls R, 1999. A shaped-beam microstrip patch reflectarray. *IEEE Trans Antenn Propag*, 47(7):1167-1173. https://doi.org/10.1109/8.785748

Prado DR, Arrebola M, Pino MR, et al., 2017. Efficient crosspolar optimization of shaped-beam dual-polarized reflectarrays using full-wave analysis for the antenna element characterization. *IEEE Trans Antenn Propag*, 65(2):623-635. https://doi.org/10.1109/TAP.2016.2633950

Rahmat-Samii Y, Michielssen E, 1999. Electromagnetic optimization by genetic algorithms. *Microw J*, 42(11):232-232.

Rahmat-Samii Y, Cramer P, Woo K, et al., 1981. Realizable feed-element patterns for multibeam reflector antenna analysis. *IEEE Trans Antenn Propag*, 29(6):961-963. https://doi.org/10.1109/TAP.1981.1142678

Robinson J, Rahmat-Samii Y, 2004. Particle swarm optimization in electromagnetics. *IEEE Trans Antenn Propag*, 52(2):397-407. https://doi.org/10.1109/TAP.2004.823969

Vacchione JD, 1990. Techniques for Analyzing Planar, Periodic Frequency Selective Surface Systems. PhD Thesis, University of Illinois at Urbana-Champaign, Illinois, USA.

Wu GB, Qu SW, Wang YX, et al., 2018. Nonuniform FSS-backed reflectarray with synthesized phase and amplitude distribution. *IEEE Trans Antenn Propag*, 66(12): 6883-6892. https://doi.org/10.1109/TAP.2018.2871752

Yu A, Yang F, Elsherbeni AZ, et al., 2009. A single layer broadband circularly polarized reflectarray based on the element rotation technique. IEEE Antennas and Propagation Society Int Symp, p.1-4. https://doi.org/10.1109/APS.2009.5171594

Zhang L, Cui Z, Jiao YC, et al., 2009. Broadband patch antenna design using differential evolution algorithm. *Microw Opt Technol Lett*, 51(7):1692-1695. https://doi.org/10.1002/mop.24423

Zhou M, Sørensen SB, Kim OS, et al., 2013. Direct optimization of printed reflectarrays for contoured beam satellite antenna applications. *IEEE Trans Antenn Propag*, 61(4): 1995-2004. https://doi.org/10.1109/TAP.2012.2232037

Zhou M, Sørensen SB, Kim OS, et al., 2014. The generalized direct optimization technique for printed reflectarrays. *IEEE Trans Antenn Propag*, 62(4):1690-1700. https://doi.org/10.1109/TAP.2013.2254446

Zhou M, Borries O, Jørgensen E, 2015. Design and optimization of a single-layer planar transmit-receive contoured beam reflectarray with enhanced performance. *IEEE Trans Antenn Propag*, 63(4):1247-1254. https://doi.org/10.1109/TAP.2014.2365039